Asian Journal of Chemistry; Vol. 26, Supplementary Issue (2014), S81-S84

ASIAN JOURNAL OF CHEMISTRY

http://dx.doi.org/10.14233/ajchem.2014.19020

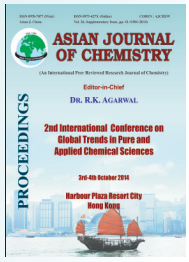

Green Synthesis of Energy Rich Petroleum Additive Over Mg-KMSU-11 Solid Acid Catalyst

CHELLAPANDIAN KANNAN* and J. ILAVARASI JEYAMALAR

Department of Chemistry, Manonmaniam Sundaranar University, Tirunelveli-627 012, India

*Corresponding author: Fax: +91 462 2322973, 2334363, Tel: +91 462 2333887; E-mail: chellapandiankannan@gmail.com

Published online: 24 December 2014; AJC-16443

Glycerol is a major byproduct in the biodiesel industries and disposal of glycerol limiting the biodiesel production. In this article, a new nano porous solid acid catalyst is developed, which converts glycerol into glycerol ether. The synthesized catalyst is characterized by various spectroscopic techniques like XRD, FT-IR, BET surface area, TGA and SEM to confirm its activity and stability. The catalyst pore size is 11 nm, it has high pore size compare to the literature report (2 to 4 nm) and also active at lower temperature (150 °C). This new material is named as Mg-KMSU-11.

Keywords: Large mesoporous, Heterogeneous catalysis, Glycerol ether, Petrol additive.

INTRODUCTION

Glycerol is a major by productin biodiesel industries[1]. The production of glycerol is considerably increased with increase of biodiesel production[2]. Glycerol has large range of applications mainly in the field of antifoaming agents, cosmetic and food industries and an additive for biofuels[3-5]. Etherification of glycerol at high temperature leads to the formation of polyglycerols. It is not suitable to add as a petrol additive. In this study, we have adapted low temperature etherification of glycerol by using Mg-KMSU-11 for the synthesis of lower molecular weight of glycerol ether which is suitable to add as a petrol additive.

EXPERIMENTAL

The Mg-KMSU-11 is prepared by using the hydrocarbon of alkyl (chain length C_{12}) as a template. The molar composition of the resultant mixture is 0.08 Na_2SiO_3 : X $MgSO_4$: 8 H_2O : 0.02 $C_{12}H_{26}$ (X-varies with the Si/Mg ratio). Sodium silicate (23 g) and magnesium sulphate are dissolved in water (140 mL) under stirring. Then template is added into the solution. The resultant mixture is stirred for 2 h at room temperature and the pH of the mixture is adjusted to 10 by the drop wise addition of concentrated sulphuric acid. The gel is aged at room temperature for 48 h and heated on hot plate to evaporate water and to attain complete crystallization of the molecular sieves. The sample is washed using distilled water and dried at 110 °C in hot air oven for 2 h. The sample is calcinated in the presence of air until all the impurities and template are completely removed from the pores of molecular sieves.

The synthesized Mg-KMSU-11 sample is characterized by using spectroscopic techniques. The low-angle X-ray diffraction (XRD) patterns are recorded on a Shimadzu 6000 diffract meter using CuK_α radiation (λ = 1.5418 Å) with the scanning rate of 0.5° per min. The fourier transform infrared (FT-IR) measurement of sample is recorded by JASCO-410 FT-IR spectrophotometer by using KBr pellet technique. Thermal analysis is carried out on SDT Q600 V8.3 build 101 at a heating rate of 20 °C/min. Nitrogen adsorption-desorption measurement is made using on Micromeritics, ASAP 2020 V3.00 H at 77 K. The scanning electron microscope analysis is performed on a JEOL JSM 6360 scanning electron microscope operated at 15 kV.

RESULTS AND DISCUSSION

Characterization of the catalyst: The FT-IR spectra of as-synthesized and calcined Mg-KMSU-11 are shown in Fig. 1a. The band appeared around 3600-3400 cm^{-1} of calcined sample is assigned the characteristic vibrations of terminal OH groups[6]. The bands appeared at 2924, 2834 and 1464 cm^{-1} is attributed to the C-H stretching modes of -CH_2 of the template molecules and these absorption bands disappear after calcination. The signals at 1043, 879 and 425 cm^{-1} are assigned to internal and external a symmetric Si-O-Si stretching modes and they are slightly shifted to higher frequencies in the calcined sample[7]. The other bands appeared below 900 cm^{-1} are mostly due to fundamental vibrations of the Mg-O-Si

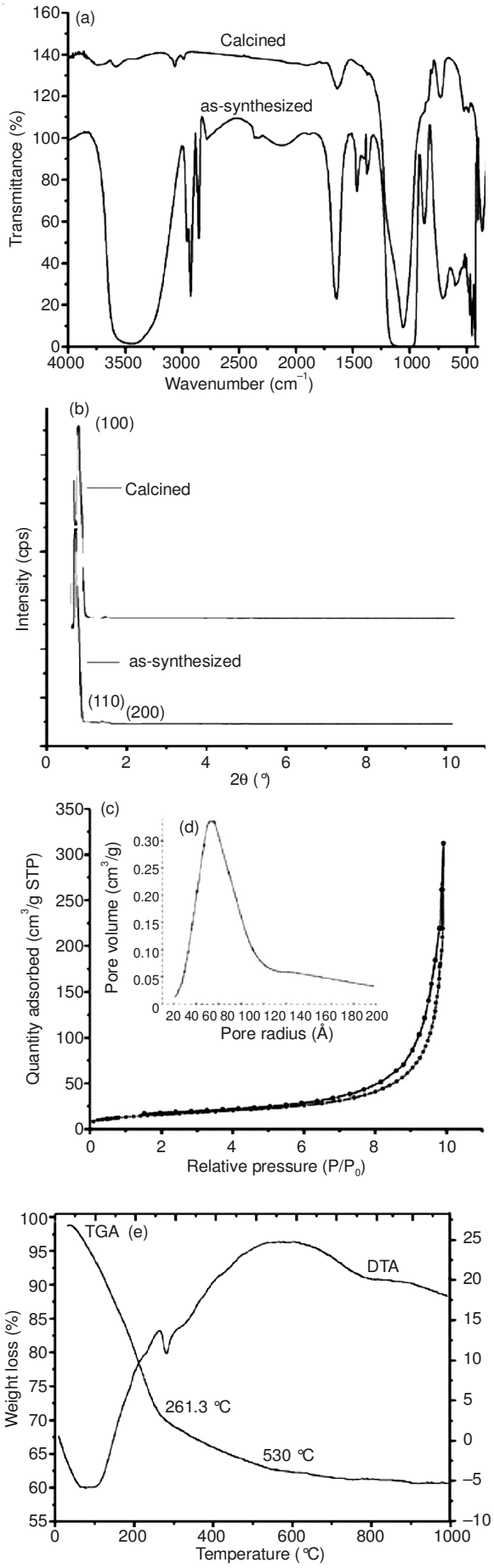

Fig. 1. Characterization results for the Mg-KMSU-11 molecular sieve

and Si-O-Si bonds in the framework. These bands appear in FT-IR proved the formation of tetrahedral framework of the molecular sieves and also the metal ion incorporation in the framework.

The X-ray powder diffraction pattern of the as-synthesized and calcined mesoporous samples are shown in Fig. 1b. Both the samples exhibited XRD patterns with high intense (100) diffraction peak and two small (110) and (200) diffraction peaks, confirming the formation of highly ordered mesostructures. The sharp primary peak around 0.8 degree of the calcined sample indicated the formation of large pore in the mesoporous material[8].

Nitrogen adsorption-desorption isotherms of the mesoporous Mg-KMSU-11 is shown in Fig. 1c. The relative pressures (P/P_0) higher than 0.5 is represented the formation of mesoporous material[9]. N_2 adsorption at low relative pressure ($P/P_0 < 0.4$) is accounted for monolayer adsorption of N_2 on the walls of the mesopores[10]. The pore volume, surface area and pore diameter Fig. 1d of calcinated Mg-KMSU-11 are 0.33 cm^3/g, 80 m^2/g and 110Å, respectively. Broadincreases of N_2 uptake in the P/P_0 range from 0.50 to 0.96 clearly indicating the wide range of mesopore formation within the tetrahedral framework of molecular sieves.

The thermogravimetric analysis of the as-synthesized molecular sieve is shown in Fig. 1e. Water desorption is observed at 100 to 120 °C[11]. The other peak appears at approximately around 260 °C indicated the removal of template from the pores (29 %). The peak appeared at the temperature range 360-550 °C with the weight loss 7.5 % is due to condensation of OH group present in the materials[12]. It has no weight loss further increased by temperature above 1000 °C means that the thermal stability of the material is above 1000 °C.

SEM image of the calcined sample is shown in Fig. 2. SEM micrograph of calcined sample is revealed the presence of well-defined spherical morphology with porous network of the agglomerated particle size range[13] from 150 to 200 nm.

Catalysis: Glycerol etherification process is performed in liquid phase. Experimental conditions like reaction time, catalyst weight, monomer dosage and temperature are optimized for maximum conversion of glycerol.

Effect of reaction time: The glycerol conversion and the selectivity of the products are shown in Fig. 3. Conversion of glycerol increased with increase of time and it attains the maximum conversion of 77 % at 6 h. The maximum diglycerol selectivity is obtained in the first 1 h and slowly decreased with increases of time. At the same time the triglycerol selectivity is increased up to 6 h and further increase of time leads the formation of polyglycerol.

Effect of temperature: The evolution of selectivity of the different glycerol ethers and the reaction progress at the varying temperature ranges from 80 to 300 °C are shown in Fig. 4. When the temperature increased, the glycerol conversion also increased and attains the maximum at 300 °C and there is no effective conversion in further increase of temperature.

The maximum diglycerol selectivity is obtained at 80 °C and decreases with increasing reaction temperature; whereas the triglycerol selectivity is increased up to 150 °C and sharply decreases while further increasing the temperature. It is found

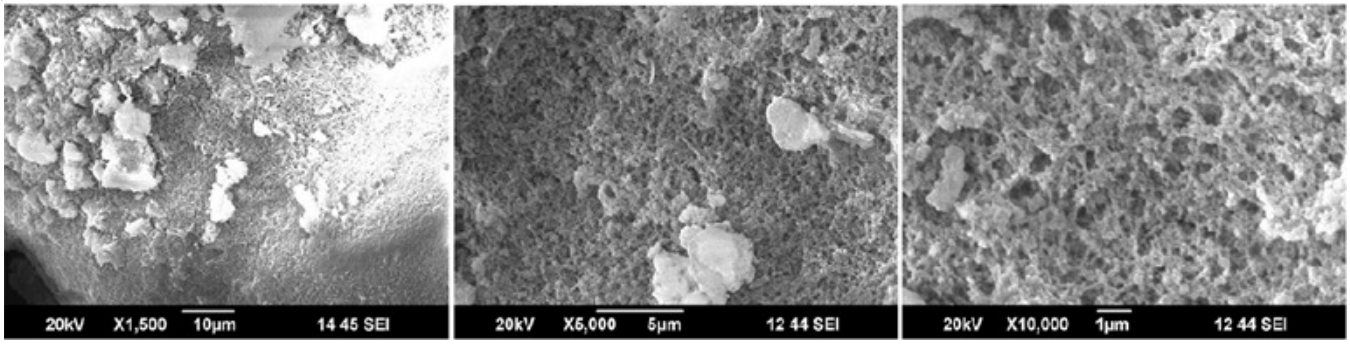

Fig. 2. SEM micrograph of mesoporous Mg-KMSU-11 molecular sieve

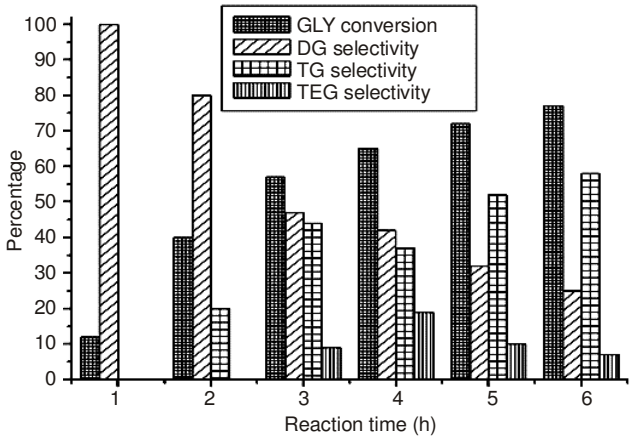

Fig. 3. Effect of contact time on glycerol etherification over mesoporous Mg-KMSU-11: Condition: 0.01 g catalyst 10 mL glycerol at 150 °C

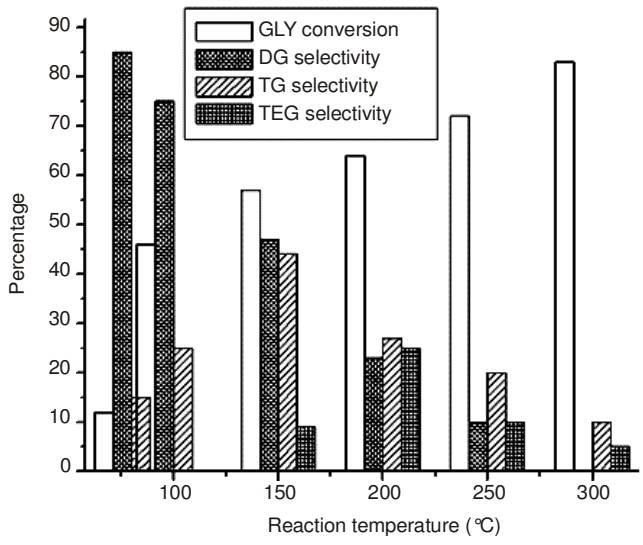

Fig. 4. Effect of temperature on glycerol etherification over mesoporous Mg-KMSU-11: Condition: 0.01 g catalyst 10 mL glycerol for 3 h

that the reaction temperature increased above 150 °C, the reaction favors the formation of poly glycerol.

Effect of catalyst loading: The effect of catalyst loading on glycerol etherification reaction over Mg-KMSU-11 molecular sieves was studied from 0.01 to 0.001 wt. % and the results were shown in Fig. 5. We have maintained the 1.26 wt. % glycerol dosage and temperature 150 °C for 3 h duration. When we decrease the dosage of catalyst, it was observed that catalytic activity also decreases whereas the diglycerol selectivity increases and *vice versa*. Since the diglycerol selectivity is not considerably decreases on increase of dosage, which reveals the active nature of this novel Mg-KMSU-11 catalyst. In case of selectivity towards triglycerol and tetraglycerol, it enhances by the increase of catalyst loading.

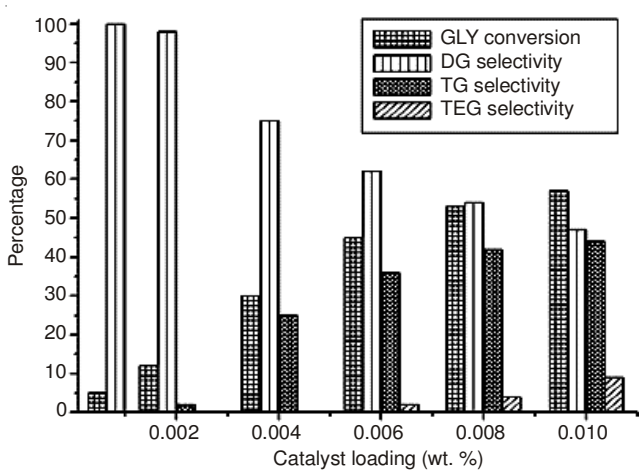

Fig. 5. Effect of catalyst loading on glycerol etherification over mesoporous Mg-KMSU-11: Condition: 10 mL of glycerol, at 150 °C for 3 h

Effect of monomer dosage: The glycerol etherification in relation to glycerol dosage is studied from 1.26 to 12.6 wt. % [10 mL = 1.26 wt. %]. The results are shown in Fig. 6. When the monomer dosage is increased, the conversion of glycerol decreased. Whereas, the diglycerol selectivity increased with

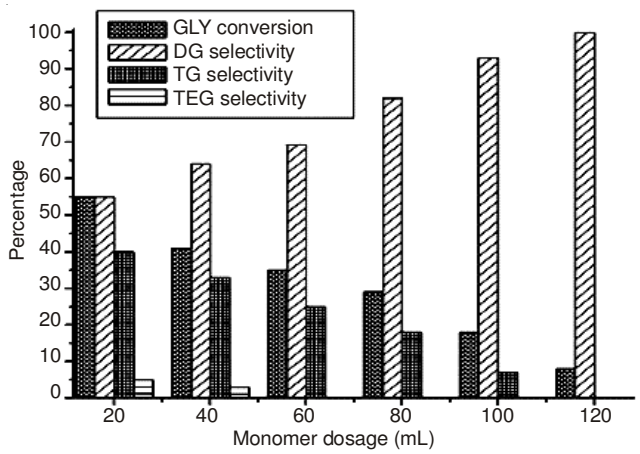

Fig. 6. Effect of monomer dosage on glycerol etherification over mesoporous Mg-KMSU-11: Condition: 0.01 g catalyst, at 150 °C, for 3 h

increase of glycerol dosage, buttriglycerol selectivity is slowly decreased. This result revealed that 1.26 wt. % glycerol is optimum for the maximum conversion.

Conclusion

A new solid acid catalyst Mg-KMSU-11 is successfully synthesized by using hydrocarbon as template. The characterization of the material proved the crystalinity, large pore size and thermal stability of the material. The catalytic activity is found to increase with increase of temperature. But higher temperature leads to the polymerization reaction. This study clearly revealed that di and tri glycerol ether selectivity are more at 150 °C. This reaction is a solvent free reaction. The catalyst is green catalyst highly active and reusable.

REFERENCES

1. M. Roze, V. Kampars, K. Teivena, R. Kampare and E. Liepins, *Mater. Sci. Appl. Chem*., **28**, 67 (2013).
2. M. Pagliaro, R. Ciriminna, H. Kimura, M. Rossi and C. Della Pina, *Eur. J. Lipid Sci. Technol*., **111**, 788 (2009).
3. A.E. Díaz-Álvarez, J. Francos, B. Lastra-Barreira, P. Crochet and V. Cadierno, *Chem. Commun.*, **47**, 6208 (2011).
4. A. Martin and M. Richter, *Eur. J. Lipid Sci. Technol*., **113**, 100 (2011).
5. J.A. Melero, R. van Grieken, G. Morales and M. Paniagua, *Energy Fuels*, **21**, 1782 (2007).
6. E. Kaya, N. Oktar, G. Karakas and K. Murtezaoglu, *Turk. J. Chem*., **34**, 935 (2010).
7. M. Tanaka, A. Itadani, Y. Kuroda and M. Iwamoto, *J. Phys. Chem. C*, **116**, 5664 (2012).
8. O.A. Anunziata, M.L. Martínez and A.R. Beltramone, *Materials*, **2**, 1508 (2009).
9. C. Kannan, K. Muthuraja and M.R. Devi, *J. Hazard. Mater*., **244-245**, 10 (2013).
10. N.N. Tušar, A. Ristic, G. Mali, M. Mazaj, I. Arcon, D. Arcon, V. Kaucic and N.Z. Logar, *Chem. Eur. J*., **16**, 5783 (2010).
11. C. Kannan, K. Sivakami and J. Ilavarasi Jeyamalar, *Mater. Lett*., **113**, 93 (2013).
12. X.-D. Li and Q.-Z. Zhai, *J. Iran. Chem. Soc*., **8(S1)**, S1 (2011).
13. H.B. Hassan, M.A. Abdel Rahim, M.W. Khalil and R.F. Mohammed, *Int. J. Electrochem. Sci*., **9**, 760 (2014).